Table 8.2: Analysis of variance (ANOVA) for the degradation of RO 16 by *Acinetobacter pitii* in terms of Concentration of dye degraded

Source	Sum of	df	Mean	F	p-value
Model	259.99	9	28.89	105.8	< 0.0001
A-pH	26.18	1	26.18	95.89	< 0.0001
B-Concentration of dye	24.11	1	24.11	88.29	< 0.0001
C-Time	23.03	1	23.03	84.33	< 0.0001
AB	0.28	1	0.28	1.03	0.3347
AC	0.57	1	0.57	2.07	0.1808
BC	3.36	1	3.36	12.31	0.0056
A^2	77.17	1	77.17	282.63	< 0.0001
B^2	7.47	1	7.47	27.34	0.0004
C^2	1.05	1	1.05	3.83	0.0789
Residual	2.73	10	0.27		
Lack of Fit	2.73	5	0.55		
Pure Error	0	5	0		
Cor Total	262.72	19			

The Quadratic model fitted best for response 1 (degradation of dye) and independent variable (Muniyasamy et al., 2020; Padmanaban et al., 2018). With the results of ANOVA, it was observed that linear terms pH (A), concentration (B) and time (C) have positive attributes, and interactive terms concentration and pH, concentration, and time have no effect but interactive term concentration and time and quadratic term time have positive attributes whereas, quadratic terms of pH and concentration have negative attributes for the response 1. The "**Predicted R-Squared**" of 0.91 was found in agreement with the "**Adjusted R-Squared**" of 0.98. The coefficient of variation is 5.09% and the **Adequate Precision** value of 32.61 a ratio greater than 4 is desirable. The relationship between the actual and predicted value of Sqrt (concentration of dye degraded) is shown in **table 8.1** and **figure8.5.**

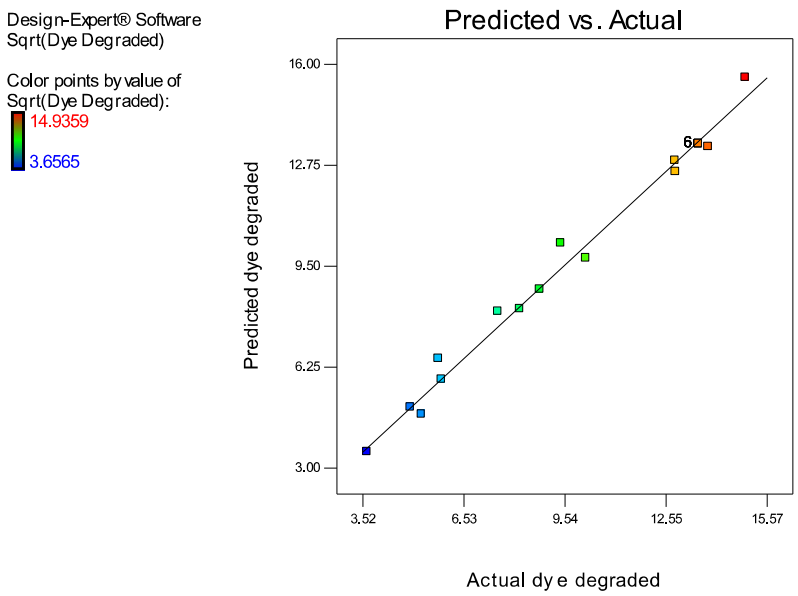

Figure 8.5 predicted vs actual data of dye degraded

- **Analysis of operational parameters of Response surface methodology**

The regression equation was used for plotting two-dimensional (contour) and three-dimensional (3D surface) for a better understanding of the interactive effects of two variables on the responses (Cho and Zoh, 2007; Jegan Durai et al., 2020; Muniyasamy et al., 2020).

(a)

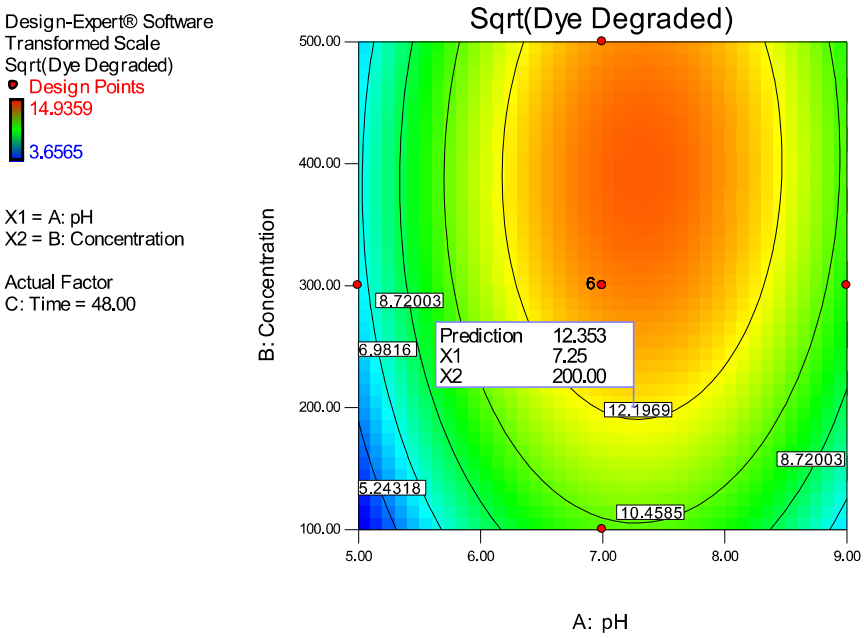
Design-Expert® Software
Transformed Scale
Sqrt(Dye Degraded)
Design Points
14.9359
3.6565
X1 = A: pH
X2 = B: Concentration
Actual Factor
C: Time = 48.00
Sqrt(Dye Degraded)
B: Concentration
A: pH
500.00
400.00
300.00
200.00
100.00
5.00
6.00
7.00
8.00
9.00
8.72003
6.9816
5.24318
12.1969
10.4585
8.72003
6
Prediction 12.353
X1 7.25
X2 200.00

(b)

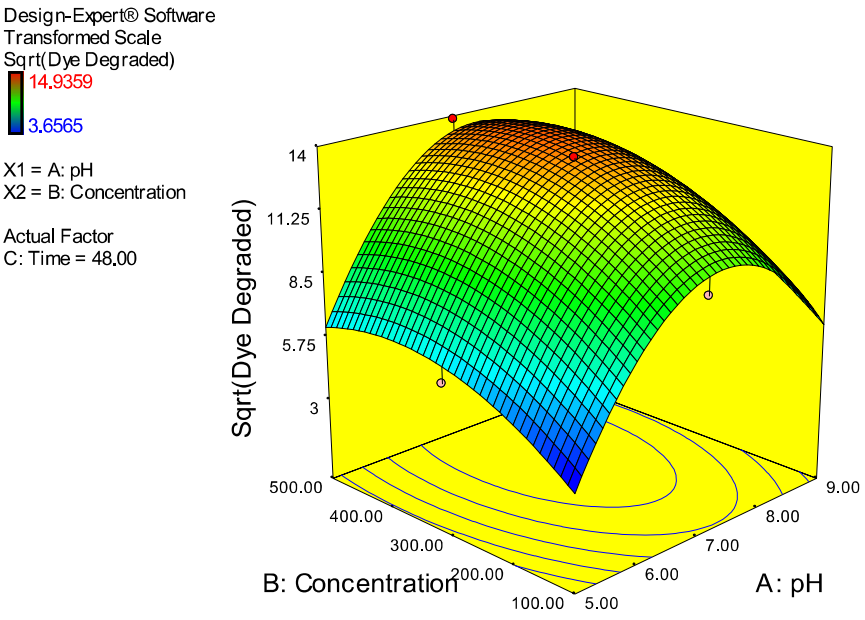
Design-Expert® Software
Transformed Scale
Sqrt(Dye Degraded)
14.9359
3.6565
X1 = A: pH
X2 = B: Concentration
Actual Factor
C: Time = 48.00
Sqrt(Dye Degraded)
14
11.25
8.5
5.75
3
B: Concentration
500.00
400.00
300.00
200.00
100.00
A: pH
5.00
6.00
7.00
8.00
9.00

(c)

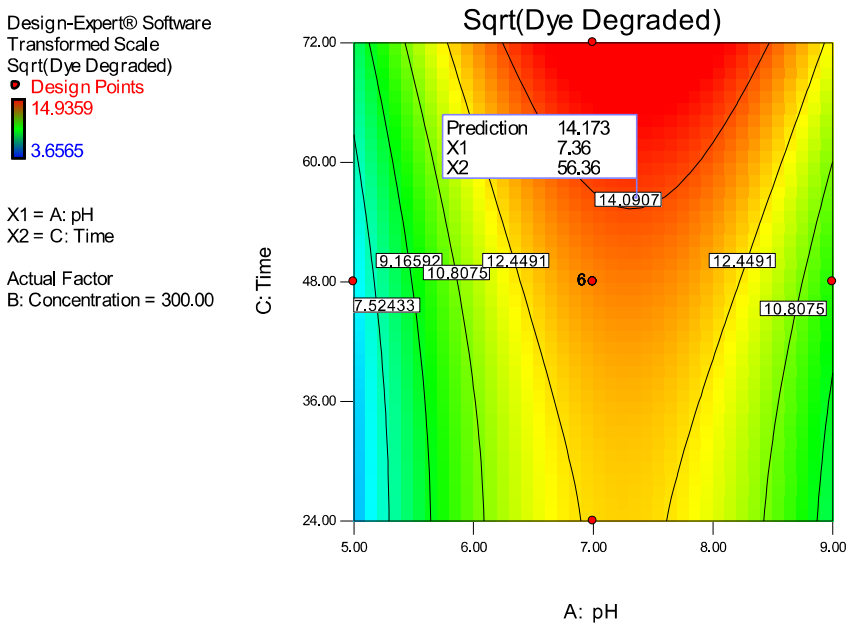
Design-Expert® Software
Transformed Scale
Sqrt(Dye Degraded)
Design Points
14.9359
3.6565
X1 = A: pH
X2 = C: Time
Actual Factor
B: Concentration = 300.00
Sqrt(Dye Degraded)
Prediction 14.173
X1 7.36
X2 56.36
14.0907
9.16592
10.8075
12.4491
12.4491
7.52433
10.8075
6
72.00
60.00
48.00
36.00
24.00
C: Time
5.00
6.00
7.00
8.00
9.00
A: pH

(d)

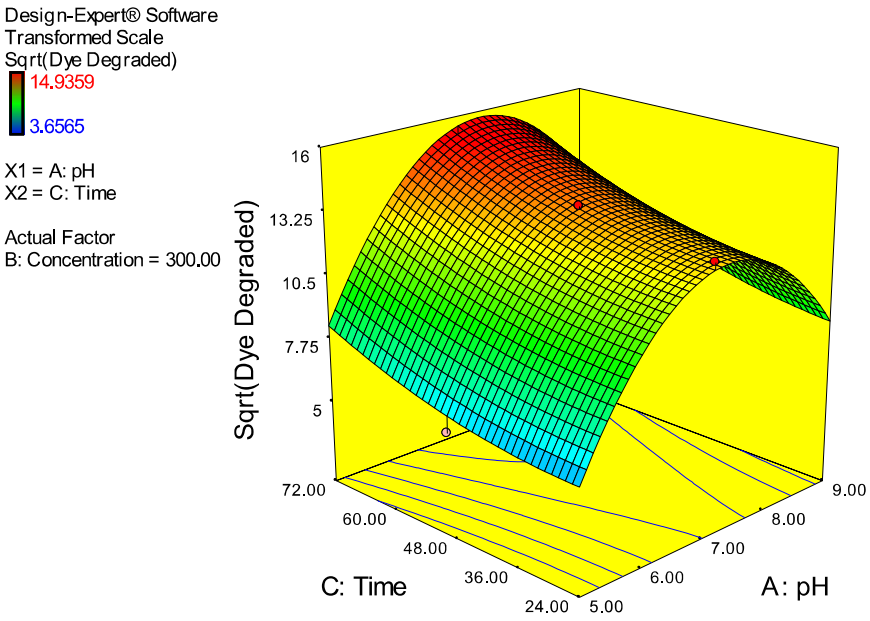
Design-Expert® Software
Transformed Scale
Sqrt(Dye Degraded)
14.9359
3.6565
X1 = A: pH
X2 = C: Time
Actual Factor
B: Concentration = 300.00
Sqrt(Dye Degraded)
16
13.25
10.5
7.75
5
72.00
60.00
48.00
36.00
24.00
C: Time
5.00
6.00
7.00
8.00
9.00
A: pH

(e)

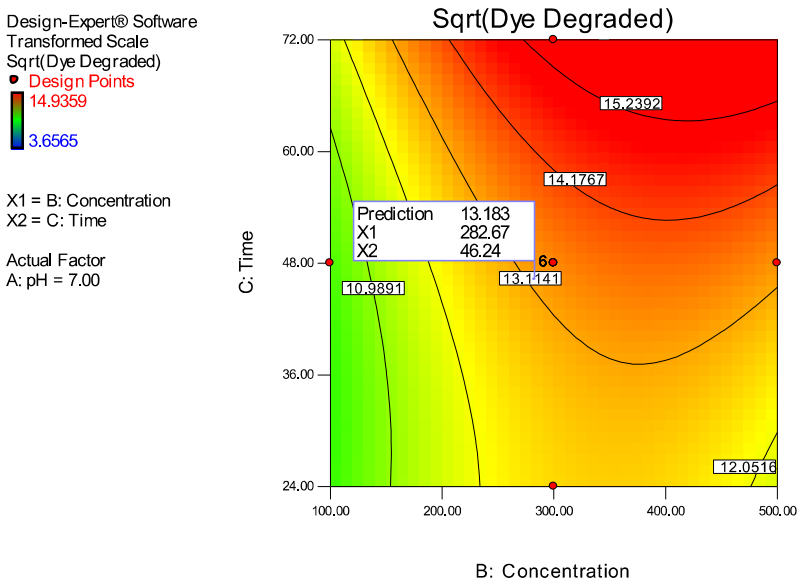

(f)

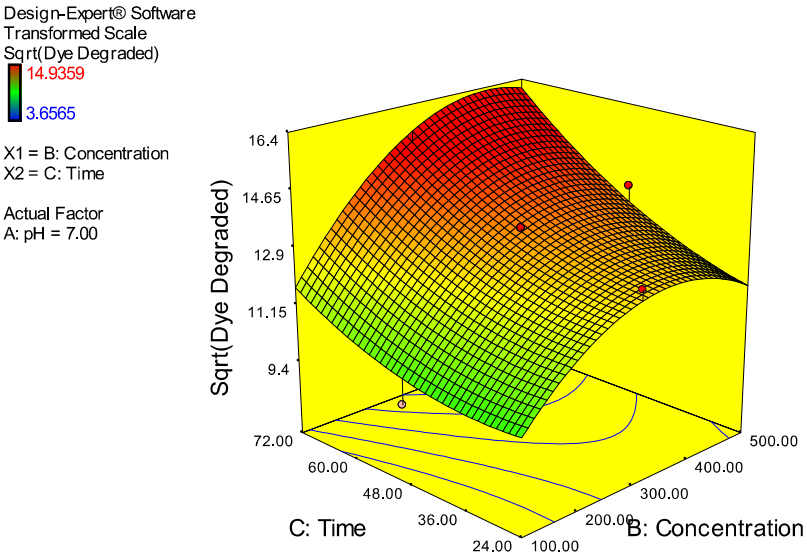

Figure 8.6 (a,b) Dye degradation as function of pH and concentration,(c,d) dye degradation as function of pH and time, (e,f) dye degradation as function of time and concentration, Figure (a,c,e) Contour plot, and (b,d,f) 3D Surface plot

From **figure 8.6(a,b),** the interactive effect between pH and concentration of dye and **figure 8.6(c,d),** the interactive effect of pH and time were not significant. **Figure 8.6 (e,f),** shows the positive interactive effect of time and concentration on dye degradation with a significant P-value <0.05. At pH 7.0, when the time was increased from 46.24 h to 58.69 h at 282 ppm initial concentration of dye, dye degradation increases from 173.79 ppm to 98.52 ppm. Similarly, when concentration was increased from 28 ppm to 395 ppm at 46.24 h, dye degradation increases from 173.91 ppm to 187.69 ppm. Overall, they have positive attributes towards dye degradation. This work is supported by previously reported literature(Kaur et al., 2015; Pazzetto et al., 2012; U. Roy et al., 2018).

- **Model response in terms of current density:**

Response 2 is for current density and its empirical relation is reduced for its significant parameters and shown in **equation 8.3.**

$$\boldsymbol{Current\ density} = -6.14 + 1.93A + 1.98B - 7.85C - 0.13A^2 - 0.000003B^2 \textbf{(8.3)}$$

Analysis of variance (ANOVA) was used to test the adequacy of the model and its results were shown in **Table 8.3**. F-value for the model was found to be 100.41 with p-values <0.05 shows that model is significant and the quadratic model is the best for response 2.

Table 8.3: Analysis of variance (ANOVA) for the degradation of RO 16 by *Acinetobacter pitii* in terms of Current density

Source	Sum of	df	Mean	F	p-value
Model	2.05	9	0.23	100.41	< 0.0001
A-pH	0.12	1	0.12	53.41	< 0.0001
B-Concentration of dye	0.034	1	0.034	14.85	0.0032
C-Time	0.042	1	0.042	18.65	0.0015
AB	1.25E-05	1	1.25E-05	5.52E-03	0.9423
AC	1.13E-04	1	1.13E-04	0.05	0.8282
BC	3.13E-04	1	3.13E-04	0.14	0.7181

A^2	0.79	1	0.79	350.36	< 0.0001
B^2	0.068	1	0.068	30.02	0.0003
C^2	9.16E-03	1	9.16E-03	4.04	0.072
Residual	0.023	10	2.27E-03		
Lack of Fit	0.023	5	4.53E-03		
Pure Error	0	5	0		
Cor Total	2.07	19			

All the interactive terms pH (A), concentration (B), and time (C), and quadratic term time have p-value> 0.05 so they can be neglected. The "**Predicted R-Squared**" of 0.89 is in reasonable agreement with the "**Adjusted R-Squared**" of 0.97 with a coefficient of variation of 7.60 % and its **Adequate Precision** value is 29.60 >4 which is desirable. The relationship between actual and predicted value current density is shown in **table8.1and figure8.7**.

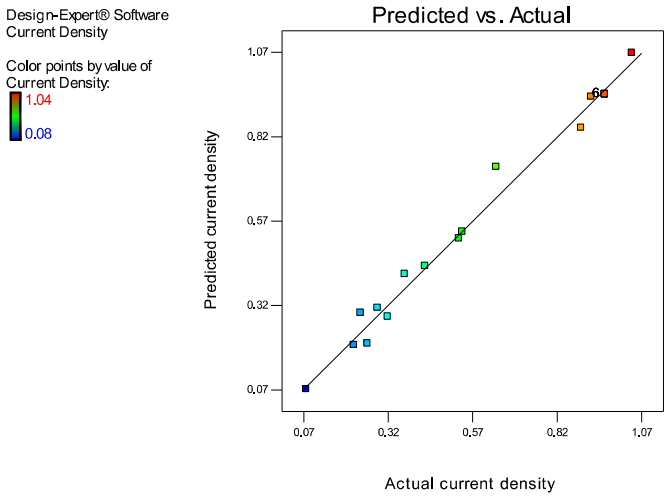

Figure 8.7 predicted vs actual data of current density

Interactive effect of pH, concentration, and time on current density

Figure 8.8 showed the 2D contour and 3D surface plot for current density. All the interactive term does not affect the response. Linear term pH and concentration have

positive effects on current density whereas linear term time and quadratic term pH and concentration have a negative effect on current density.

(a)

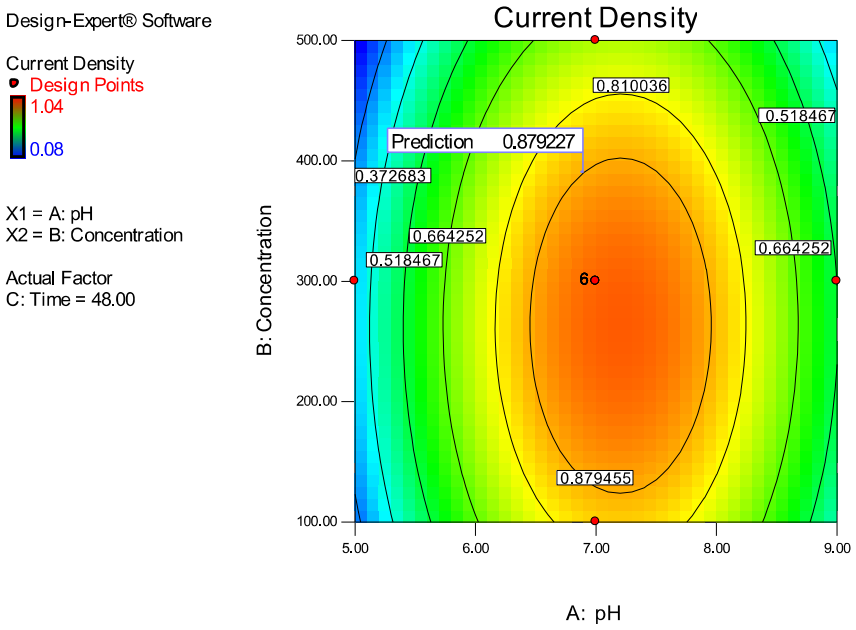

(b)

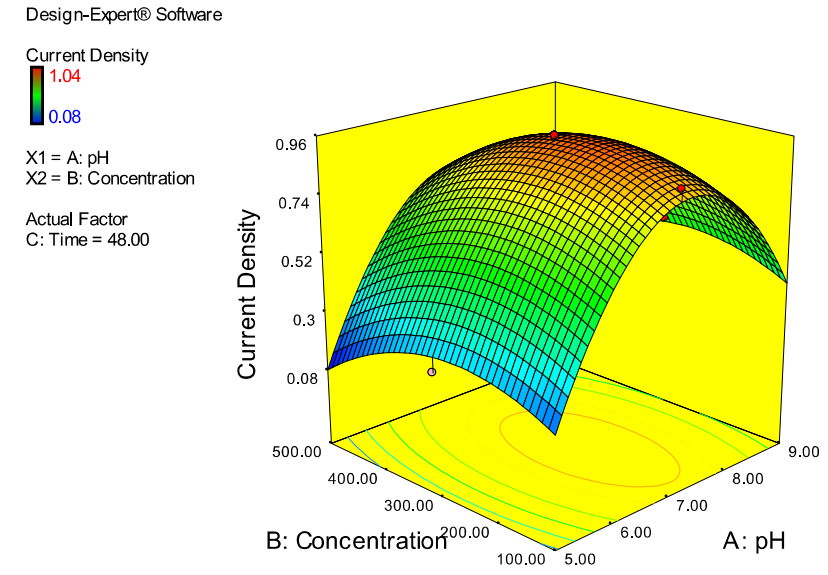

(c)

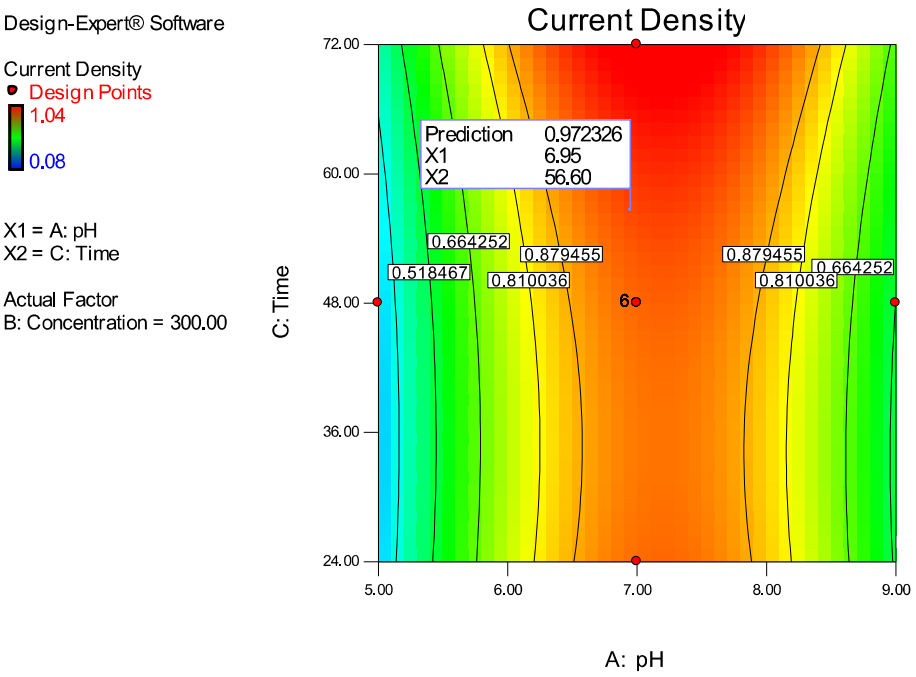
Design-Expert® Software
Current Density
Design Points
1.04
0.08
X1 = A: pH
X2 = C: Time
Actual Factor
B: Concentration = 300.00
Current Density
Prediction 0.972326
X1 6.95
X2 56.60
0.664252
0.879455
0.518467
0.810036
0.879455
0.664252
0.810036
6
72.00
60.00
48.00
36.00
24.00
C: Time
5.00
6.00
7.00
8.00
9.00
A: pH

(d)

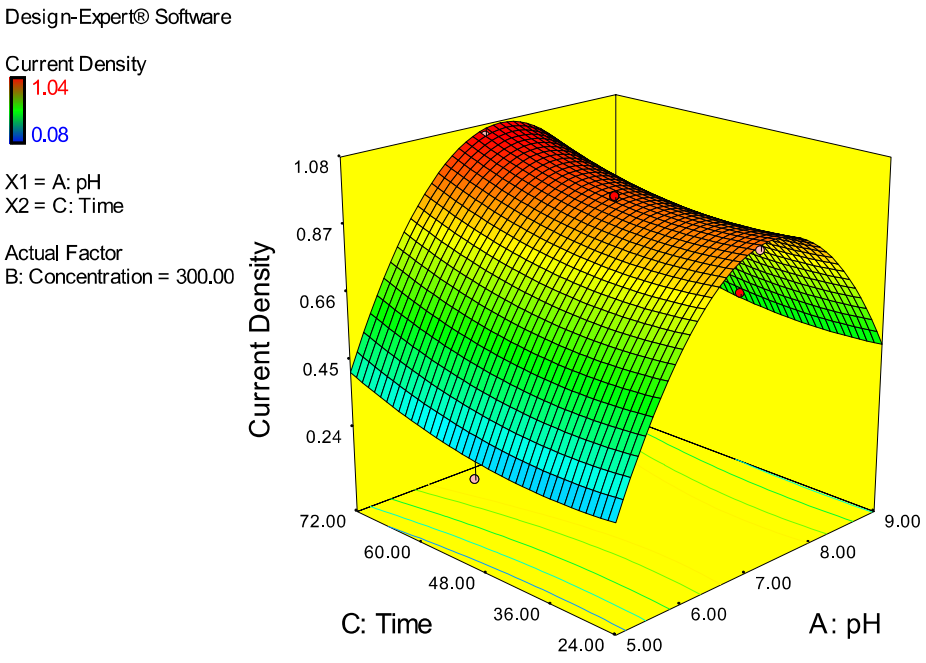
Design-Expert® Software
Current Density
1.04
0.08
X1 = A: pH
X2 = C: Time
Actual Factor
B: Concentration = 300.00
Current Density
1.08
0.87
0.66
0.45
0.24
72.00
60.00
48.00
36.00
24.00
C: Time
5.00
6.00
7.00
8.00
9.00
A: pH

(e)

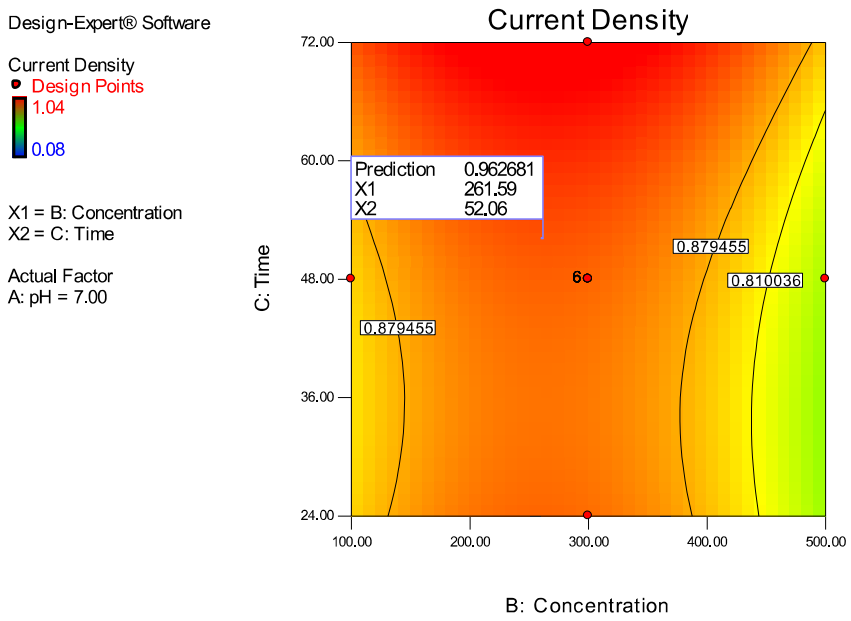

(f)

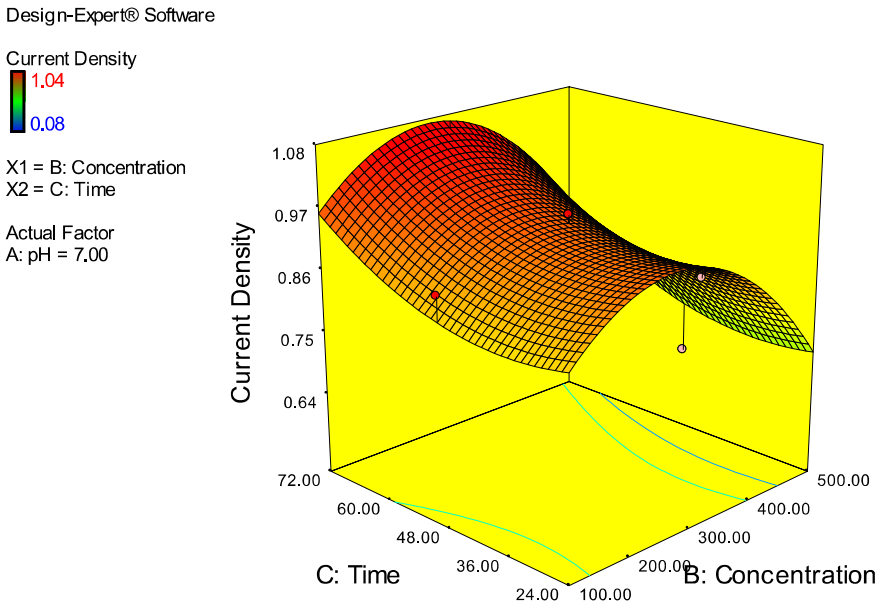

Figure 8.8 (a,b)current density as function of pH and concentration,5(c,d) current density as function of pH and time,5 (e,f) current density as function of time and concentration, Figure (a,c,e) Contour plot, and 4 (b,d,f) 3D Surface plot

- **Optimized numerical solutions for degradation of dye and current density**

Various responses along with their variables were optimized and solutions are given in **Table 8.4.** Variables like pH, concentration, and time were kept in the range while response degradation of dye and current density were maximized using an optimization technique. From the various solution, when the pH was kept 7.35 with a concentration of dye 295.06 in 71.27 h resulted in maximum dye degradation of 243.17 ppm with the 1.06 A/m^3 current density. A quadratic model was found to be the best fit for these parameters. The predicted and actual response (**Table 8.1**) has an error of ±0.5%, which suggests that the model is suitable for predicting the behavior of dye in the microbial fuel cell**.**

Table 8.4 optimized numerical solutions for degradation of dye and current density

No.	pH	The concentration of dye (ppm)	Time (h)	Sqrt(Conc. of Dye Decolorised)	Conc. of Dye Decolorised (ppm)	Current Density (A/m^3)
1	7.16	330.13	70.57	15.81	249.9561	1.05126
2	7.35	295.06	71.27	15.594	243.1728	1.06676
3	7.23	331.97	69.72	15.76	248.3776	1.04454
4	7.39	349	71.8	16.157	261.0486	1.04561
5	7.22	343.15	70.32	15.91	253.1281	1.04269
6	7.32	328.79	71.62	15.974	255.1687	1.05858

- **Analysis of degraded metabolites of RR 120**

Functional group identification using FTIR analysis

Figures 8.9 (a) and (b) represent the % transmittance of control dye and its metabolites after degradation in the microbial fuel cell. In figure 6(a), the peaks at 3741.09 cm^{-1}

showed -OH stretching of benzene substituted alcohol. -NH stretching and >C=O stretching of the amide of RO 16 were obtained at the peaks of 3439.96 cm^{-1} and 1722.10 cm^{-1}. The peaks at 1657.68 cm^{-1}, 1640.60 $cm^{-1,}$ and 1631.16 cm^{-1} correspond to -N=N- stretching of the azo bond, >C=O stretching vibration, and –NH bending of amide group present in RO 16. The peaks obtained between 1512.88 cm^{-1} to 1563.99 cm^{-1} were because of –CH bending and –C=C- stretching of aromatic ring present in RO 16. The peak present at 1483.42 cm^{-1} was due to aromatic ring stretching of RO 16 and the peak at 1461.67 cm^{-1} was due to >S=O stretching of SO_2 molecule. The peak at 1432.44 cm^{-1} and 1110.41 cm^{-1}corresponds to para-substituted azobenzene and -OH stretching of -SO_3H group present in RO 16 dye respectively. The peak at 617.92 cm^{-1} and 499.68 cm^{-1} represented the fingerprint region and correspond to the -OH out of plane bending vibration and -C=C- out of plane ring bending of RO 16. When the results of FTIR spectrums of control reactive orange 16 (**Figure 8.9(a))** are compared with degraded RO 16 (**Figure 8.9(b)**), we observed no missing peaks and shifting of the peaks. This indicates the successful biodegradation of dye in the microbial fuel cell. In **figure 8.9(b),** 3444.47 cm^{-1} peak corresponds to -NH stretching of the amide with a small shift in peak from -NH stretching of RO 16. 1634.61 cm^{-1} also showed –NH bending of the amide with a small shift from 1631.16 cm^{-1} to 1634.61 cm^{-1}. The absence of any spectra between 1400 cm^{-1} to 1550 cm^{-1} confirmed the breakdown of the aromatic ring of RO 16. Also, the absence of a peak at 1657cm^{-1} in the metabolic compound confirmed the breakdown of characteristics azo bond of RO 16. The peak obtained at 1401.23 cm^{-1} and 1079.68 cm^{-1} was due to C-H deformation and conversion of secondary alcohol of RO 16 to a primary alcohol. The peak shifts and generation of new peaks confirmed the biodegradation of RO 16 in microbial fuel cells (Bheemaraddi et al., 2014; Saha and Rao, 2019; Shobana and hangam, 2012).

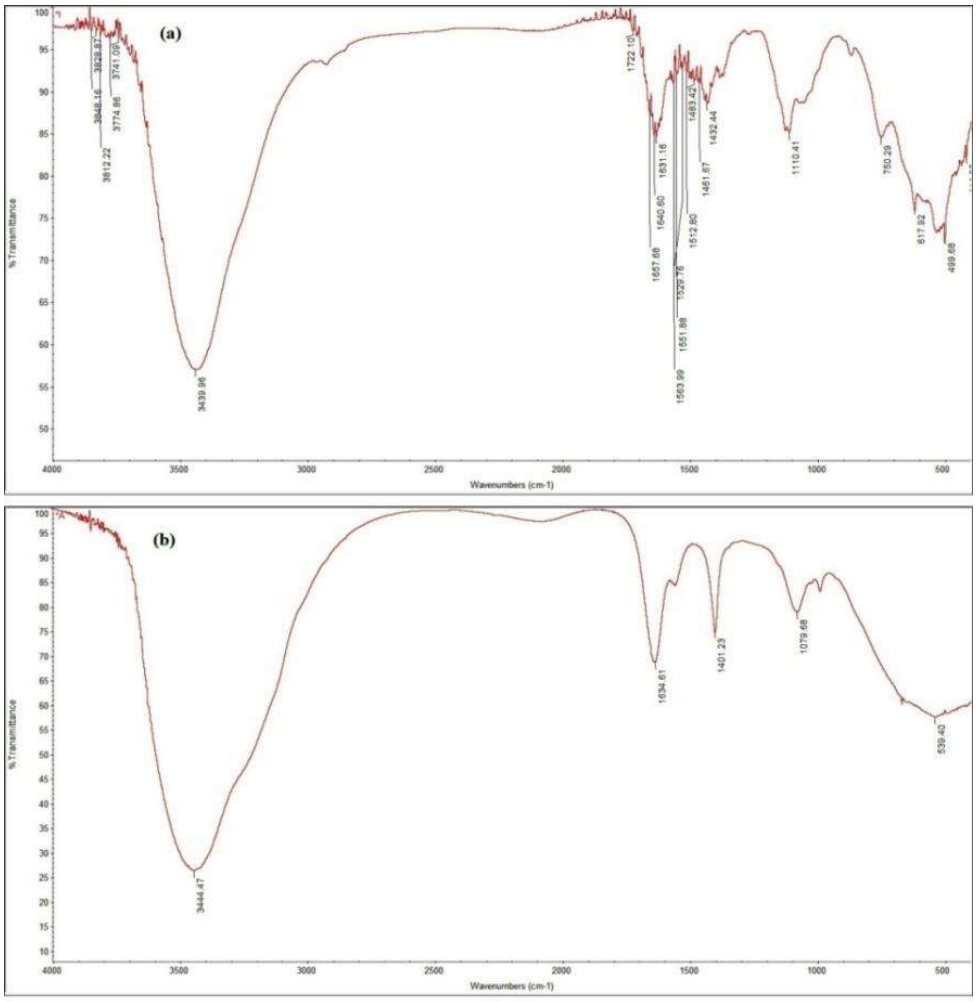

Figure8.9 (a) FTIR spectrums of control reactive orange 16 and (b) decolorized reactive orange 16

Degradation pathway using LCMS analysis

LCMS analysis of biodegraded dye in the microbial fuel cell was done to know the possible, stable metabolites of dye after its bio-oxidative breakdown in the microbial fuel cell. LCMS spectra for RO 16 dye (Appendix 1)showed peaks at m/z 474.5 and m/z 594.2 were due to vinyl and hydrolyzed form of RO 16 dye (Svobodová et al., 2007). Some stable and known compounds were detected and confirmed by the NIST library. The compounds confirmed by the NIST library are 2-Methyl-4-nitrobenzene sulfonic

acid (m/z 217.2) and2-Amino-3-hydroxynaphthalene-1-sulfonic acid (m/z 239.2). These compounds are possibly formed by the cleavage of the characteristic azo bond of RO 16 dyes. They are further degraded to lower molecular weight unstable aldehyde compounds by opening their ring structure (Shobana and hangam, 2012). The degradation pathway of dye mainly depends on bacterial species and many factors that is why the researchers have reported the formation of different compounds such as 1-amino-1-naphthalene sulphonic acid (m/z 223), 6-acetamido- 3,4-dioxo-3,4-dihydro naphthalene-2-sulfonate (m/z 294), (E)-2-(4-acetamidophenyl)-1-carboxyethensulfonate(m/z284),4-(2-hydroxyethylsulfonyl)phenolate (m/z 201), 6- acetamido naphthol -2- sulfonic acid (m/z 279), 6- nitroso naphthol(m/z 170) during biodegradation of dyes(Saha and Rao, 2019; Shobana and hangam, 2012; Šlosarčíková et al., 2020; Svobodová et al., 2007). Based on FTIR and LCMS results, a biodegradation pathway was proposed for the degradation of RO 16 and shown in **figure 8.10**. The complete catabolic pathway of RO 16 dye degraded products has to be studied. However, obtained amino derivatives are reported to be used for the bacteria catabolic pathway for its carbon and energy needs, which could be responsible for its mineralization (Fernando et al., 2014a).

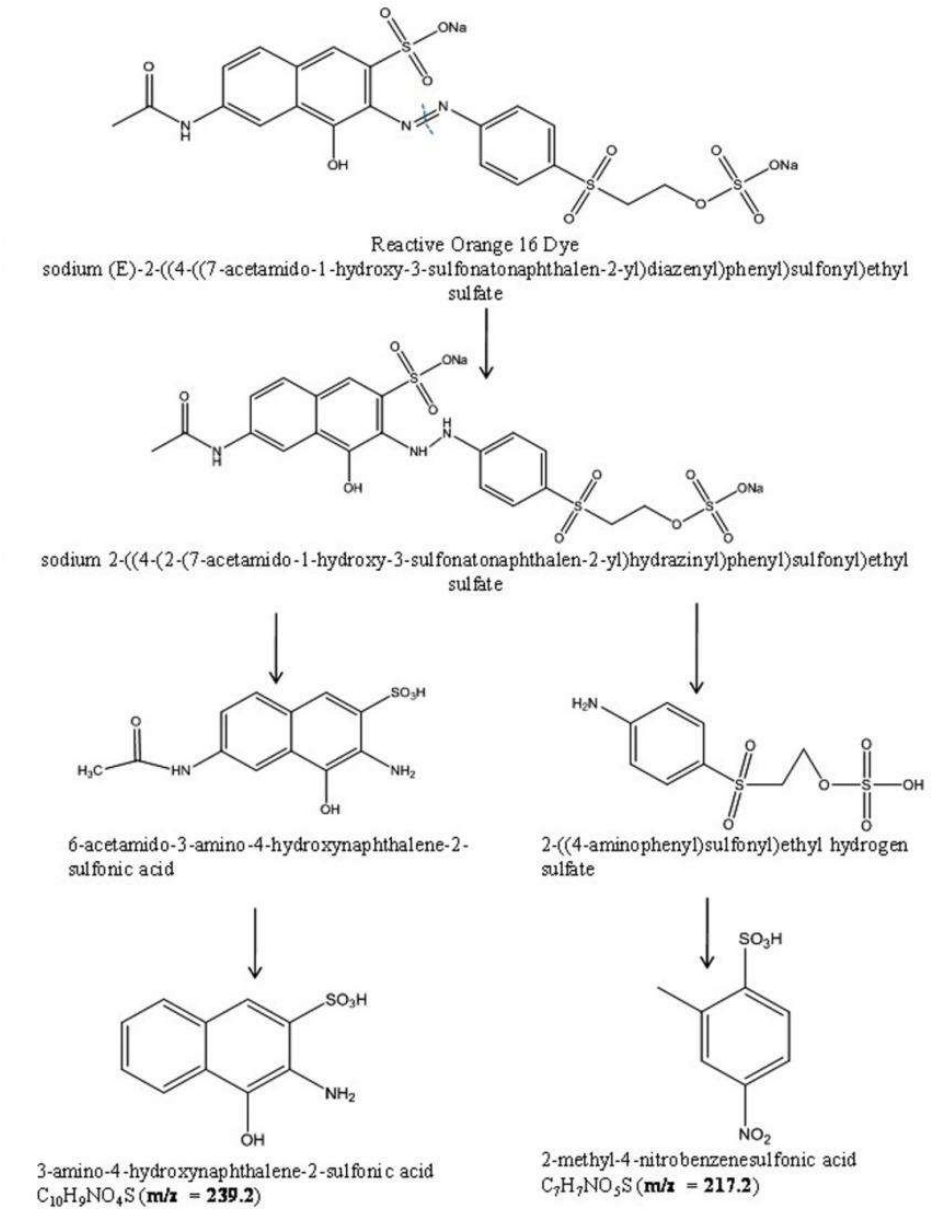

Figure8.10 Proposed biodegradation pathway for reactive orange 16 degradations by *Acinetobacter pitii*

- **Coulombic efficiency (%CE)**

At the end of the experiment %, CE was calculated and found to be 2.29 % for *Acinetobacter pitii* and 2.07% for mixed culture for 500 dye concentration at 1000Ω resistance. A very low value indicated that most of the electron released during dye

degradation was not only utilized for electricity production, rather utilized for biomass growth and other metabolites (Koroglu et al., 2016; Sulonen et al., 2014; M. Zhang et al., 2019)

- **Phytotoxicity studies**

Phytotoxicity studies are shown in **figure 8.11**. % Germination in the case of control(distilled water) and treated RO 16 dye wastewater were found higher than RO 16 dye wastewater. All the seeds were germinated in the case of control and treated dye wastewater. The length of the plume and radical in treated dye wastewater was more than untreated dye, which showed that toxicity was reduced significantly after the treatment of dye wastewater in the microbial fuel cell. But the length of plume and radical in control was higher than treated dye wastewater this may be attributed to the presence of intermediates due to dye degradation.

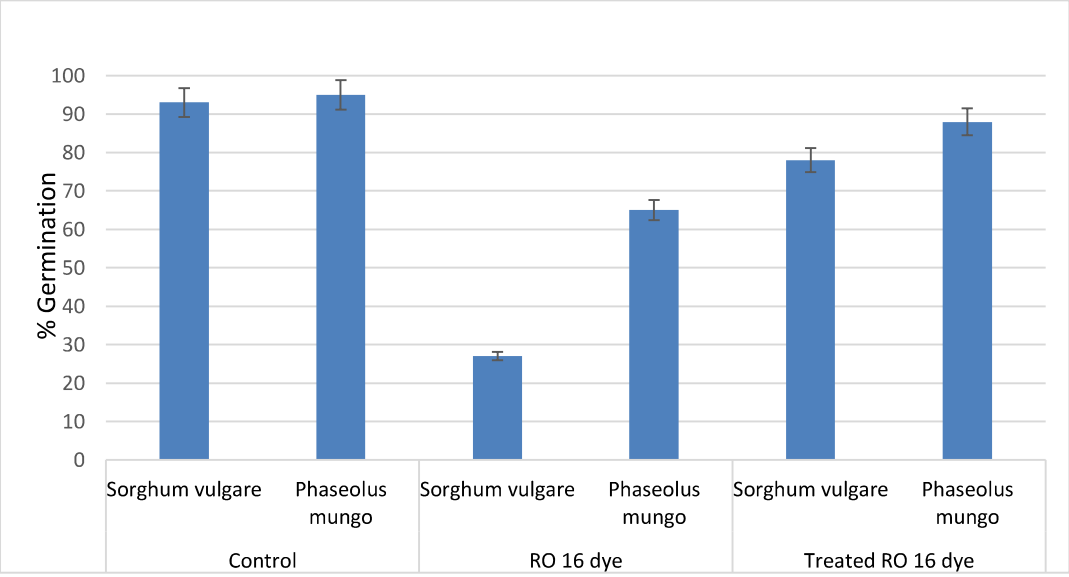

Figure 8.11 Phytotoxicity study

8.1.3 Concluding Remarks

The present study successfully demonstrates the successful degradation of Reactive Orange 16 dye in the microbial fuel cell along with simultaneous electricity production. SEM results indicated the successful growth of bacterial species. The biodegradation of Orange 16 dye was confirmed by the results of FTIR, LCMS, CO_2 production, COD, and color removal. The microbial fuel cell inoculated with *Acinetobacter pitii* performed better as compared to mixed-species microbial fuel cells. More than 80% COD and 90% color removal were obtained under steady-state in the microbial fuel cell inoculated with *Acinetobacter pitii* . The quadratic model was found to be best suited to the experiment with a p-value <0.05. 3D Response surface plot showed the significant interactive effect of all three parameters on the dye degradation and current density. Through the Box-Cox design, parameters were optimized. RSM results were obtained very well in agreement with the experimental results with an error of ±0.5%. The Phytotoxicity results indicated a significant reduction in the toxicity of degraded dye, and it can be used for irrigation purposes. The electricity production in the microbial fuel cell was in line with other researchers, but there should be more research to improve it for possible commercialization. The % Columbic efficiency indicated that only 2 to 3 % electron generated during bio-oxidation was utilized for electricity production, and the rest were used in the other biological routes. The result indicated possible enhancement potential in terms of electricity production.